DOE/ET/53088-60 IFSR #60

# Solitary Drift Waves in the Presence of Magnetic Shear

J. D. Meiss
and
W. Horton

Institute for Fusion Studies
The University of Texas at Austin
Austin, Texas 78712

July 1982

# SOLITARY DRIFT WAVES IN THE PRESENCE OF MAGNETIC SHEAR

J. D. Meiss
and
W. Horton

Institute for Fusion Studies
The University of Texas at Austin
Austin, Texas 78712



Abstract

The two-component fluid equations describing electron drift and ion acoustic waves in a nonuniform magnetized plasma are shown to possess nonlinear two-dimensional solitary wave solutions. In the presence of magnetic shear, radiative shear damping is exponentially small in $L_s/L_n$ for solitary drift waves, in contrast to linear waves.

## I. INTRODUCTION

Nonlinearity in the equations for drift waves in a nonuniform, magnetized plasma permits the formation of solitary waves in addition to the usual small amplitude dispersive modes. By analogy with the well known Korteweg de Vries equation in one dimension, drift wave dispersion and nonlinear steepening (mode coupling) can balance to form coherent structures localized in the plane perpendicular to $\underset{\sim}{B}$. These localized solutions of the drift wave equations are called solitary vortices or modons (pronounced mōd-ons).

Two important physical properties of solitary drift waves are that they propagate with speeds complementary to the speeds of the linear modes, and that they possess a high degree of stability to perturbations and self-collisions. Recently,[1] these features of one-dimensional solitons were used to construct a drift wave turbulence theory based on an ideal gas approximation for an ensemble of drift wave solitons. The dynamical form factor $S(k,\omega)$ of a one-dimensional drift wave soliton gas has features that are qualitatively different from those derived from weak turbulence theory.

In the present work, the theory of two-dimensional solitary drift waves in the presence of a sheared magnetic field is developed. After a brief treatment of the two-dimensional solitary drift waves in the straight magnetic field using techniques[2-4] developed for nonlinear atmospheric waves, it is shown that the effect of shear on the solitary drift waves is fundamentally different from that on the linear waves.[5] In the sheared system, the nonlinearity of the wave equation produces an effective potential well that reflects the outward propagating wave energy. For small amplitude solitary waves the potential well is weak;

however, for finite amplitude solitary waves the radial well is deep and only an exponentially small outgoing wave tunnels through the barrier. Due to the nonlinear barrier, the radiative shear induced damping of the solitary drift wave is exponentially small for modons propagating either faster than the electron diamagnetic drift velocity or in the ion diamagnetic direction.

To further characterize the drift wave dynamics, as would be measured in fluctuation experiments, we compute the dynamical form factor $S(\underset{\sim}{k},\omega)$ for a uniformly-distributed collection of identical modons. Due to the strong coherence of solitary waves, the frequency-integrated wavenumber spectrum $S(\underset{\sim}{k})$ has a maximum at finite $\underset{\sim}{k}_\perp$ and a power law behavior for large $k_\perp$. For a distribution[6] of solitary waves with varying energies, such as the Gibbs ensemble, the frequency spectrum at fixed $\underset{\sim}{k}_\perp$ becomes broad and peaked at frequencies above the electron diamagnetic frequency $\omega_{*e}$.

The article is organized as follows: In Sec. II the two-component fluid equations are reduced and the conservation laws are derived. In Sec. III the solitary vortex solutions are derived following the analysis of Flierl et al.[4] and generalized to include $k_\parallel \neq 0$. Some recent atmospheric simulations showing the stability of the vortex are noted. In Sec. IV the dynamical form factor of a uniform ensemble of two-dimensional solitary drift waves is given. In Sec. V the solutions of the three-dimensional drift wave equation in the presence of magnetic shear is derived. In Sec. VI we provide the conclusions.

## II. EQUATION OF MOTION

We consider electrostatic electron drift waves and ion acoustic waves in the inhomogeneous plasma slab $n_0(x)$ with a sheared magnetic field $\underset{\sim}{\Omega} = (eB/m_i c)(\hat{z} + x\hat{y}/L_s)$ . The dynamical equations are the pressureless ion fluid and the almost adiabatic electron fluid equations. The condition of quasi-neutrality relates the ion density to the electron density $n(\underset{\sim}{x},t)$ which is taken to be

$$\ell n\tilde{n} = \ell n \frac{n(\underset{\sim}{x},t)}{n_0(x)} = (1 + \mathscr{L})\phi(\underset{\sim}{x},t) \tag{1}$$

where $\phi = e\Phi/T_e$ is the normalized electrostatic potential and $\mathscr{L}$ is an operator giving the nonadiabatic part of the electron response.

The ion fluid equations can be written

$$\frac{D}{Dt}\ell n\tilde{n} - \frac{v_x}{L_n} + \nabla \cdot \underset{\sim}{v} = 0 \tag{2}$$

$$\frac{D}{Dt}\underset{\sim}{v} = -c_s^2\nabla\phi + \underset{\sim}{v} \times \underset{\sim}{\Omega} \quad , \tag{3}$$

where $L_n^{-1} = -\partial_x \ell n n_0(x)$ , $c_s^2 = T_e/m_i$ , and

$$\frac{D}{Dt} = \frac{\partial}{\partial t} + \underset{\sim}{v} \cdot \nabla \quad .$$

An ordering for the drift waves consistent with experimental evidence of low-frequency fluctuations is given by

$$\varepsilon \equiv \frac{\rho_s}{L_n} \sim \frac{\omega}{\Omega} \sim \frac{v}{c_s} \sim \phi \ll 1 \qquad (4)$$

where $\rho_s = c_s/\Omega$ and $\omega$ represents a typical frequency. An additional but independent small parameter is

$$S \equiv \frac{L_n}{L_s} ,$$

measuring the density gradient scale compared with the scale for rotation of the magnetic field vector. The rotation of the magnetic field vector couples the ion acoustic oscillations to the drift waves and implies the ordering

$$k_\parallel L_n \sim k_\perp \rho_s \sim \mathcal{O}(1) . \qquad (5)$$

This ordering for $k_\parallel$ is in contrast to that of Hasegawa and Mima[7] where $k_\parallel L_n \sim \mathcal{O}(\varepsilon)$ justifies the neglect of the parallel ion oscillations.

With the orderings Eqs. (4) and (5), the natural dimensionless variables are

$$\begin{aligned} \underset{\sim}{x}_\perp &\to \rho_s \underset{\sim}{x}_\perp \\ z &\to L_n z \\ \phi &\to \varepsilon\phi \\ \underset{\sim}{v}/c_s &\to \varepsilon \underset{\sim}{v} \\ t &\to (L_n/c_s)t , \end{aligned} \qquad (6)$$

where the variables on the left-hand side of these equations are the physical variables and those on the right-hand side are used subsequently.

Resolving momentum balance in the x-y plane and $\hat{z}$-direction, we can solve Eq. (3) for $\underset{\sim}{v}_\perp = (\hat{z} \times \underset{\sim}{v}) \times \hat{z}$ and for $v_z$ to obtain

$$\underset{\sim}{v}_\perp = \hat{z} \times \nabla_\perp \phi - \varepsilon \frac{D}{Dt} \nabla_\perp \phi + \varepsilon S x v_z \hat{y} + \mathcal{O}(\varepsilon^2, \varepsilon^2 S)$$

$$\frac{Dv_z}{Dt} = - \frac{\partial \phi}{\partial z} + S x v_x \ , \tag{7}$$

where

$$\frac{D}{Dt} = \frac{\partial}{\partial t} + \hat{z} \times \nabla \phi \cdot \nabla + \mathcal{O}(\varepsilon, \varepsilon S) = \frac{\partial}{\partial t} + [\phi, \ ] \ . \tag{8}$$

In the convective derivative, the incompressible $\underset{\sim}{E} \times \underset{\sim}{B}$ flow dominates and is written in terms of the Jacobian or Poisson brackets defined by

$$[a,b] = \frac{\partial a}{\partial x} \frac{\partial b}{\partial y} - \frac{\partial a}{\partial y} \frac{\partial b}{\partial x} \ .$$

With these velocity fields the continuity equation [Eq. (2)] and Eq. (7) become to lowest order in $\varepsilon$ and $S$

$$\frac{D}{Dt}\left(1 + \mathscr{L} - \nabla_\perp^2\right)\phi + v_d \frac{\partial \phi}{\partial y} + \hat{b} \cdot \nabla v_z = 0 \ . \tag{9a}$$

$$\frac{Dv_z}{Dt} = - \hat{b} \cdot \nabla \phi \tag{9b}$$

where $\hat{b} \cdot \nabla = \frac{\partial}{\partial z} + Sx \frac{\partial}{\partial y}$ . The linear dispersion relation of Eq. (9) in

the absence of shear is given by $\omega^2(1 + \mathscr{L}_{\underset{\sim}{k\omega}} + k_\perp^2) - \omega k_y v_d - k_\parallel^2 c_s^2 = 0$ where $v_d = \rho_s c_s / L_n = 1$ and $\mathscr{L}_{\underset{\sim}{k\omega}}$ is the Fourier transform representation of the operator $\mathscr{L}$ .

For systems with sufficiently weak shear $[S < \mathcal{O}(\varepsilon)]$ the coupling of the drift wave to the ion acoustic wave may be neglected. Taking $\hat{b}\cdot\nabla \sim ik_\parallel = 0$ and neglecting the non-adiabatic electron response, $\mathscr{L} = 0$ in Eq. (1), Eq. (9) reduces to that derived by Hasegawa and Mima[7]

$$\frac{D}{Dt}(1 - \nabla_\perp^2)\phi + v_d \frac{\partial \phi}{\partial y} = 0 . \tag{10}$$

It is interesting to note that Eq. (10) is the expression of Ertel's theorem[8] on conservation of potential vorticity through $(\varepsilon^2)$ (see Appendix). Equation (10) was first derived by Charney[9] in a geophysical context for Rossby waves in a rotating neutral fluid. The analogy between Rossby waves and drift waves has been discussed by Hasegawa, Maclennan and Kodama.[10]

The drift wave energy density and the enstrophy are defined by

$$E = \frac{1}{2}\int d^3x \left[\phi^2 + (\nabla_\perp \phi)^2 + v_z^2\right] \tag{11}$$

$$K = \frac{1}{2}\int d^3x \left[(\nabla_\perp \phi)^2 + (\nabla_\perp^2 \phi)^2\right] . \tag{12}$$

These quantities are conserved in the $k_\parallel = 0$ dynamics of Eq. (10) but not by the full dynamics of Eqs. (8) and (9). The energy and enstrophy change due to electron dissipation and to radiative damping from shear-induced ion acoustic waves:

$$\frac{dE}{dt} = -\int d^3x\phi \frac{D}{Dt}\mathscr{L}\phi + \int dydz\ \phi \left.\frac{\partial^2\phi}{\partial x \partial t}\right|_{x=-L}^{x=L} . \tag{13a}$$

$$\frac{dK}{dt} = \int d^3x \nabla_\perp^2\phi \left(\frac{D}{Dt}\mathscr{L}\phi + \hat{b}\cdot\nabla v_z\right) + \int dydz \frac{\partial\phi}{\partial x}\left(\frac{\partial\phi}{\partial t} + \frac{\partial\phi}{\partial y}\right)\Bigg|_{x=-L}^{x=L} . \tag{13b}$$

The fields $\phi(\underset{\sim}{x},t)$ and $v_z(\underset{\sim}{x},t)$ are assumed to decay as $y$, $z \to \infty$ (or to be periodic). They are, generally, finite at large $x$ due to magnetic shear,[5] and the last term in Eq. (13) represents linear radiative damping. We will see in Sec. V that the nonlinearity may be neglected in the radiation region for a solitary drift wave. In addition, the enstrophy is not conserved due to the coupling of the cross-field motion with the compressible parallel motion.

## III. SOLITARY DRIFT WAVE VORTICIES: SHEARLESS CASE

A solitary vortex or modon solution of the Charney equation[9] was discovered by Stern[2] and Larichev and Reznik.[3] In this section we follow the exposition of Flierl *et al.*[4] to obtain a solitary vortex from Eqs. (8), and (9) with $k_\parallel \neq 0$ but $S = \mathscr{L} = 0$.

Traveling wave solutions of Eqs. (8) and (9) are obtained by letting $\eta = y + \alpha z - ct$ and looking for solutions of the form

$$\begin{aligned} \phi(x,y,z,t) &= \phi(x,\eta) \\ v_z(x,y,z,t) &= v_z(x,\eta) \end{aligned} \tag{14}$$

where $c$ is the speed of propagation. Using Eqs. (14), it is easy to see that

$$v_z(x,\eta) = \frac{\alpha}{c}\,\phi(x,\eta) \tag{15}$$

satisfies Eq. (9b) exactly, since $[\phi, v_z] = 0$ . Substituting Eqs. (14) and (15) into Eq. (9a) with $\mathscr{L} = 0$ yields a nonlinear partial differential equation for $\phi(x,\eta)$ which can be written as a single Poisson bracket relation:

$$\left[\phi - cx,\ \nabla_\perp^2\phi - \phi + \left(v_d + \frac{\alpha^2}{c}\right)x\right] = 0 \ . \tag{16}$$

This relationship implies that the functions in the bracket are dependent,

$$\nabla_\perp^2\phi - \phi + \left(v_d + \frac{\alpha^2}{c}\right)x = F(\phi - cx) \ , \tag{17}$$

where F is an arbitrary function. We are looking for localized solutions, that is for each $x$ , $\phi \to 0$ as $y \to \infty$. Considering the $y \to \infty$ limit of Eq. (17) determines the form of $F$ :

$$F(z) = -\left(\frac{v_d}{c} + \frac{\alpha^2}{c^2}\right)z \ , \tag{18}$$

that is, F must be linear for localized solutions. Note that the result in Eq. (18) is not an approximation, but results from the requirement that the solution be localized with the form $\phi(x,\eta)$ . Using Eq. (18) for $F$ in Eq. (17) gives

$$\nabla_\perp^2\phi + \left(\frac{v_d}{c} - 1 + \frac{\alpha^2}{c^2}\right)\phi = 0 . \tag{19}$$

Isolation of the solution requires that the speed of the vortex satisfy

$$c^2 - cv_d - \alpha^2 > 0 . \tag{20}$$

It is important to note that the linear modes $\exp(i\underset{\sim}{k} \cdot \underset{\sim}{x} - i\omega t)$ have phase velocities $\omega/k_y$ which obey the opposite condition from inequality in Eq. (20). Figure 1 shows the allowed regions for the localized, nonlinear solutions called solitary waves. The solutions with $c > v_d$ are nonlinear electron drift waves, while solutions with $c < 0$ are nonlinear ion acoustic waves retarded by the density gradient $v_d$ and rotating in the ion diamagnetic direction.

Equation (19) has solutions which are a sum of modified Bessel functions. At present we follow Flierl et al.[4] and consider only one mode in this sum

$$\phi = AK_1\left(\frac{\beta r}{a}\right)\cos\theta$$

$$r^2 \equiv x^2 + \eta^2 \qquad \text{and} \qquad \cos\theta \equiv x/r$$

$$\beta = a\left(1 - \frac{v_d}{c} - \frac{\alpha^2}{c^2}\right)^{1/2} . \tag{21}$$

At this point we notice that there exist contours of the function $\psi = \phi - cx$ which do not extend to $y \to \infty$. On these closed contours the function $F(\psi)$ of Eq. (17) cannot be determined by the argument leading to Eq. (18). For the single mode solution, closed contours occur within

the circle of radius r = a defined by $\psi = 0$ . Within this circle the function F may be chosen arbitrarily subject to the requirement that $\phi$ be twice differentiable across the boundary.

The simplest choice of F(z) in the interior is

$$F^{int}(z) = -\left(\frac{\gamma^2}{a^2} + 1\right) z \quad .$$

Continuity of $\phi$ , $\partial\phi/\partial r$ and $\nabla_\perp^2\phi$ at r = a determines the solution

$$\phi(r,\theta) = \begin{cases} AK_1\left(\frac{\beta r}{a}\right) \cos\theta & \text{for } r > a \\ \\ \frac{Br}{a}\cos\theta + CJ_1\left(\frac{\gamma r}{a}\right)\cos\theta & \text{for } r < a \quad . \end{cases} \tag{22}$$

$$A = \frac{ac}{K_1(\beta)} , \qquad B = ac\left(1 + \frac{\beta^2}{\gamma^2}\right) , \qquad C = -\left(\frac{\beta}{\gamma}\right)^2 \frac{ac}{J_1(\gamma)}$$

and $\gamma$ is determined by

$$\frac{K_2(\beta)}{\beta K_1(\beta)} = -\frac{J_2(\gamma)}{\gamma J_1(\gamma)} \equiv \delta \quad . \tag{23}$$

Equation (23) has an infinite set of roots $\gamma_n(\beta)$ , n = 1,2,..., as shown in Fig. 2. As $\beta \to 0$ the roots $\gamma_n$ become the nth zero of $J_1(\gamma_n)$ while as $\beta \to \infty$ they become the nth zero of $J_2(\gamma_n)$ . Thus, the

variation of a particular $\gamma_n$ over the entire range of $\beta$ is of order $\pi/2$ .

In this vortex dipole solution, Eqs. (22) and (23), the parameters $a$ , $c$ , and $\alpha$ or $A$ , $c$ , and $\alpha$ may be chosen independently subject to the inequality in Eq. (20). All other parameters in Eq. (22) are determined for a specified branch of Eq. (23).

The exterior form of the solution is determined by $\beta/a$ and is thus independent of the matching across the boundary at $r = a$ as well as the form of $F^{int}(\psi)$ . However, the stability of the solitary vortex may depend strongly on the form of $F^{int}(\psi)$ : a theorem[11] of Arnold implies that flow in a bounded domain obeying Eq. (17) is stable if $dF/d\psi < 0$ .

Numerical experiments imply that the modon solution with $\gamma = \gamma_1(\beta)$ is stable, though it probably does not have the extreme stability of a soliton. McWilliams et al.[12] subjected the modon to random initial perturbations and found that it survived if the RMS perturbation amplitude was less than 10-20 per cent of the modon amplitude. For larger perturbations the modon was destroyed by the shearing of its contours in the ambient (applied) field. Experiments on collisions of modons[13] show that for some parameter ranges coaxial collisions are nearly elastic. More generally, internal degrees of freedom seem to be excited by the collisions and fission or filamentation of the dipoles is possible.

There have apparently been fewer computations involving the higher mode, e.g., $\gamma_2(\beta)$ , $\gamma_3(\beta)$ , etc., solitary vortices, although it seems reasonable to suppose these will be less stable than the first mode. Aref[14] has shown a collision between a $\gamma_2(\beta)$ and a $\gamma_1(\beta)$ vortex for

the 2-D Euler equations in which the $\gamma_1$ vortex absorbs the nucleus of the $\gamma_2$ vortex, leaving what appears to be two first mode vortices.

Fleirl et al.[4] have shown that the solution in Eq. (22) can be generalized by the addition of a azimuthally-symmetric "rider" field. The radial structure of this field is determined by matching conditions at r = a as before, but its amplitude can be chosen arbitrarily. Thus, it is possible for the azimuthally-symmetric term to mask the cos θ nature of the modon.

## IV. MODON PROPERTIES

In this section we obtain the modon amplitude, size, energy, enstrophy, and spectrum as a function of the parameters a and c . For simplicity, we set $\alpha = 0$ .

### A. Asymptotic Forms

Consider first the limiting form of $\phi$ for small and large values of $\beta$ . From Eq. (23) we obtain the asymptotic forms of the parameter $\delta$ :

$$\delta \sim \begin{cases} \dfrac{2}{\beta^2} - \log\beta + 0.11593 + \mathcal{O}(\beta^2, \beta^2\log\beta) \quad , & \beta << 1 \\ \dfrac{1}{\beta} + \dfrac{3}{2\beta^2} + \mathcal{O}\left(\dfrac{1}{\beta^3}\right) \quad , & \beta >> 1 \quad . \end{cases}$$

Using this we obtain expressions for $\gamma(\beta)$

$$\gamma_n(\beta) \sim \begin{cases} \gamma_n^0 \left[1 + \dfrac{\beta^2}{2(\gamma_n^0)^2}\right] + \mathcal{O}(\beta^4, \beta^4 \log\beta) \ , & \beta \ll 1 \\ \gamma^\infty{}_n \left(1 - \dfrac{2}{\beta} + \dfrac{7}{\beta^2}\right) + \mathcal{O}\left(\dfrac{1}{\beta^3}\right) \ , & \beta \gg 1 \ , \end{cases}$$

where $\gamma_n^0$ and $\gamma_n^\infty$ are defined as the nth zeros of $J_1$ and $J_2$, respectively.

The limit $c \to v_d$ with a fixed (so that $\beta \to 0$) is the Eulerian limit of the Charney equation, since the electron streaming term exactly cancels the drift term leaving precisely the vorticity equation for a two-dimensional Eulerian fluid.

In this limit the modon reduces to a vortex pair solution given by Batchelor[15]

$$\phi_E = \begin{cases} \dfrac{a^2 v_d}{r} \cos\theta & r > a \\ \\ a v_d \left[\dfrac{r}{a} - \dfrac{2}{\gamma_n^0} \dfrac{J_1(\gamma_n^0 r/a)}{J_0(\gamma_n^0)}\right] \cos\theta & r < a \ . \end{cases} \tag{24}$$

This solution looks like a point vortex dipole for $r > a$.

In the opposite limit, $c \to 0^-$ with a fixed (so that $\beta \to \infty$) the modon becomes

$$\phi_S = \begin{cases} 0 & r > a \\ \dfrac{a^3 v_d}{\gamma_n^\infty}\left[\dfrac{J_1(\gamma_n r/a)}{J_1(\gamma_n^\infty)} - \dfrac{r}{a}\right]\cos\theta & r < a \end{cases} \tag{25}$$

as was first obtained by Stern.[2] Here the nonlinearity acts to completely screen the dipole for $r > a$ .

B. Modon Size and Amplitude

Defining the actual size of the modon, $r_0$ , as the radius at which $\phi$ is maximum gives

$$J_1'\left(\gamma \frac{r_0}{a}\right) = \frac{1}{\gamma} J_1(\gamma)\left(1 + \frac{\gamma^2}{\beta^2}\right)$$

which is graphed in Fig. 3(a) for $a = 1$ .

In the limits of large and small $\beta$ , $r_0$ takes the values

$$\frac{r_0}{a} = \begin{cases} 0.55 & \beta \to 0 \\ 0.32 & \beta \to \infty \ . \end{cases} \tag{26a}$$

The peak amplitude, shown in Fig. 3(b) for $a = 1$ , varies as

$$\phi(r_0) \simeq \begin{cases} 1.28ac & \beta \to 0 \\ \\ 0.076a^3(c - v_d) & \beta \to \infty \end{cases} . \qquad (26b)$$

Note that for a given radius, $a$, the electron modon ($c > v_d$) requires a finite amplitude field for creation, $\phi > 1.28\, av_d$.

C. Spectral Distribution

Electromagnetic scattering experiments in confinement devices measure the electron density fluctuations through the dynamical form factor $S(\underset{\sim}{k},\omega)$. The observed spectra are approximately isotropic in $\underset{\sim}{k}_\perp$ and peaked in $k_\perp$ near $k_\perp \rho_s \lesssim 1/2$. For each $\underset{\sim}{k}_\perp$ the frequency distribution is peaked at $\omega_p \gtrsim \omega_{*e}$ with a width $\Delta\omega > \omega_p$.

The fluctuation spectrum of a uniform distribution of $N_s$ identical modons is given by

$$S(\underset{\sim}{k},\omega)\delta(\underset{\sim}{k} - \underset{\sim}{k}')\delta(\omega - \omega') = \frac{1}{(2\pi)^4}\left\langle \phi(\underset{\sim}{k},\omega)\phi^*(\underset{\sim}{k}',\omega') \right\rangle$$

where $\phi(\underset{\sim}{k},\omega) = \int d^3x dt \exp(-i\underset{\sim}{k} \cdot \underset{\sim}{x} + i\omega t)\phi(\underset{\sim}{x},t)$ and the average is over the initial position $\underset{\sim}{x}_0$ of the modons. The Fourier transform of Eq. (22) gives

$$S(\underset{\sim}{k},\omega) = \frac{(2\pi)^3 N_s}{V}\left[ ca^2\beta^2(\beta^2 + \gamma^2)\,\frac{k_x}{k_\perp^2}\,\frac{J_2(k_\perp a) + \delta k_\perp a J_1(k_\perp a)}{(\beta + k_\perp^2 a^2)(\gamma^2 - k_\perp^2 a^2)}\right]^2$$

$$\times\, \delta(\omega - k_y c)\delta(k_z - \alpha k_y) . \qquad (27)$$

The spectrum is isotropic in $\underset{\sim}{k}_\perp$ except for the factor $k_x/k_\perp$ due to the dipole nature of the modon. Since the modon propagates at a fixed speed, only frequencies satisfying the dispersion relation $\omega = k_y c$ are excited. Figure 4 shows $S(k_\perp) = \int dk_z d\omega\ S(\underset{\sim}{k},\omega)$ for $k_y = 0$. In this graph the spectrum is peaked at $ka = 0.54$ and decays as $k^{-9}$ for $ka \gg 1$ with oscillations due to the Bessel functions in Eq. (27).

A more general state consisting of a superposition of modons with various sizes and speeds will have a spectrum given by Eq. (27) with $N_s$ replaced by a sum over the individual parameters (a,c). This spectrum will have a frequency width proportional to the spread in velocity of the modon ensemble.

D. Energy and Enstrophy

The modon energy and enstrophy integrals can be computed straightforwardly. For $k_\parallel = \alpha = 0$ we obtain

$$E = L_c \frac{\pi a^4 c^2}{4} \left[1 + \left(\frac{\beta}{\gamma}\right)^2\right] \left\{(\delta\beta)^2 + (4\delta + 1)\left[\frac{3}{2}\left(\frac{\beta}{\gamma}\right)^2 + \frac{1}{2} - \frac{v_d}{c}\right]\right\}$$

$$K = L_c \frac{\pi a^2 c^2}{4} \beta^2 \left[1 + \left(\frac{\beta}{\gamma}\right)^2\right] \left[\left(\frac{\beta\gamma\delta}{a}\right)^2 + 4\delta + 1\right], \qquad (28)$$

where $L_c$ is the effective length of the physical system containing the two dimensional structure.

These formulas are shown in Fig. 5. The asymptotic forms for large and small $\beta$ are

$$E \simeq \begin{cases} 2\pi a^2 c^2 L_c \left[1 + \frac{a^2}{4}(.3616 - \log\beta)\right] & \beta \to 0 \\ \frac{\pi a^8}{4\gamma^4} L_c \left(c - v_d\right)^2 \left[\left(\frac{\gamma}{a}\right)^2 + \frac{3}{2}\right] & \beta \to \infty \end{cases} \tag{29}$$

$$K \simeq \begin{cases} \pi a^2 c^2 L_c \left[2 + \left(\frac{\gamma}{a}\right)^2\right] & \beta \to 0 \\ \frac{\pi a^6}{4\gamma^2} L_c \left(c - v_d\right)^2 & \beta \to \infty \quad . \end{cases} \tag{30}$$

The energy of the Eulerian vortex dipole ($\beta = 0$) is infinite because of the slow fall off of $\phi(\propto 1/r)$ as $r \to \infty$ . This property implies that there is a modon with $c > v_d$ with minimum energy for a given $a$ . As an example when $a = 1$, $E_{min} = 10.2\ L_c$ at $c = 1.04 v_d$ while at $a = 10.0$, $E_{min} = 2.2(10^4) L_c$ at $c = 1.008 v_d$. This contrasts with the one-dimensional analogue of the modon: solitary wave solutions of the Petviashvili equation.[6] For these solutions the energy of the $c > v_d$ branch goes to zero as $c \to v_d$ while the $c < 0$ branch has a minimum energy state for $c \simeq -0.1 v_d$ .

## V. SHEAR DAMPING OF SOLITARY DRIFT WAVES

In this section, we consider the effect of variable pitch in the magnetic field on a solitary wave localized near a rational surface. Letting $x = 0$ represent this surface, we take $\hat{b}(x) = \hat{z} + \hat{y}(x/L_s)$ . The sheared field induces a distribution of values for $\alpha = k_\parallel / k_y \sim x/L_s$ which, in linear theory, produces a strong damping[5] of drift waves and convective cells. This theory predicts that a linear mode localized near $x = 0$ will spread radially. The energy radiated to large $x$ is effectively lost from the waves by ion Landau damping at $x \sim x_i \simeq \rho_s/S$ by the resonance $k_\parallel(x_i)v_i = \omega$ .

A drift wave modon, however, is localized about some point $x = x_0$ , due to the nonlinear coupling terms, and becomes exponentially small for $|x - x_0| \gg a$ . If we suppose that $x_0$ and $a$ are small compared to $x_T \simeq \rho_s/S^{1/2}$ , the Pearlstein-Berk turning point, then the effects of shear are small in the regions where the modon amplitude is substantial. Shear is important in the region $|x - x_0| \gg a$ where linear theory is valid.

The modon can be thought of as a nonlinear antenna. We obtain the radiation field due to this antenna by matching the linear solution to the modon solution in the region $a \ll |x - x_0| \ll x_T$ where both shear and nonlinearity are unimportant. For $a/\rho_s \ll S^{-1/2}$ there is a region of overlap of the two solutions which validates the asymptotic matching.

The nonadiabatic electron response, represented by the operator $\mathscr{L}$ in Eq. (1), is also modified by shear. If $\mathscr{L}$ represents electron Landau resonance, then it is nonzero only in the region $|x| \lesssim x_e \simeq S^{-1}(m_e/m_i)^{1/2}$ . If the modon is located at a position $x_0 \gg x_e$ , then $\mathscr{L}$ can also be treated using linear theory. If,

however, the modon is placed at the rational surface, then nonlinear effects must be considered in treating the electron response. This latter problem is a difficult one which we leave for later work.

Temporarily neglecting $\mathscr{L}$, we first treat the region far from the modon. For simplicity, we set $x_0 = 0$, though the modon can be positioned at any $x_0 \ll x_T$, giving $\alpha = x_0/L_s$ as the effective $k_\parallel$ its neighborhood, without substantially changing the results.

Linear solutions are obtained by discarding the advective terms in Eq. (9) and Fourier transforming in y and t. This yields the familiar eigenmode equation

$$\frac{\partial^2}{\partial x^2} \phi_{k_y\omega}(x) + Q(x)\phi_{k_y\omega}(x) = 0$$

where

$$\begin{aligned} Q(x) &= E - V(x) \\ E &= \frac{k_y v_d}{\omega} - 1 - k_y^2 \\ V(x) &= -\left(S \frac{k_y v_d}{\omega} x\right)^2 . \end{aligned} \tag{31}$$

The WKB solution of Eq. (31) has turning points at

$$|x| = x_T = S^{-1} \left|\frac{\omega}{k_y v_d}\right| (-E)^{1/2} , \tag{32}$$

which are on the real axis for $E < 0$ , as we will see is the case for modons. The WKB solutions of Eq. (31) are, for $x > 0$ ,

$$\phi_{k_y\omega}(x) = \begin{cases} \mathcal{A}_{k_y\omega}\left[-Q(x)\right]^{-1/4} \exp\left\{\mp \frac{i\pi}{4} + \int_x^{x_T}\left[-Q(x')\right]^{1/2}dx'\right\}, & x < x_T \quad (33a) \\ \mathcal{A}_{k_y\omega}\left[Q(x)\right]^{-1/4} \exp\left\{\pm i\int_{x_T}^{x}\left[Q(x')\right]^{1/2}dx'\right\}, & x > x_T. \quad (33b) \end{cases}$$

In the region $a << x << x_T$, $\phi_{k_y\omega}(x)$ in Eq. (33) must match the drift wave modon which, from Eq. (22), has the form

$$\phi(x,y - ct) \cong A\left(\frac{a\pi}{2\beta r}\right)^{1/2} \exp\left(-\frac{\beta r}{a}\right) \cos\theta \ , \qquad (34)$$

for $\beta r/a >> 1$, where $r = \left[x^2 + (y - ct)^2\right]^{1/2}$ . Fourier transformation of Eq. (34) in y and t using a saddle point approximation which is valid for $\beta x/a >> 1$ gives

$$\phi_{k_y\omega}(x) = \delta(\omega - k_y c)\frac{\pi a}{\beta} A \exp\left[-|x|\left(1 + k_y^2 - \frac{v_d}{c}\right)^{1/2}\right] . \qquad (35)$$

Matching Eqs. (33a) and (35) is accomplished by expanding Q(x) in Eq. (33a) for $x << x_T$ .

It is immediately clear from Eq. (35) that only frequencies $\omega = k_y c$ are excited. Once we set $\omega$ to this value, the functional dependence of $\phi_{k_y\omega}$ on x is the same in the two solutions. The radiation amplitude becomes

$$\mathcal{A}_{k_y\omega} = \delta(\omega - k_y c)\frac{\pi a}{\beta} A \left(1 + k_y^2 - \frac{v_d}{c}\right)^{1/4} \exp\left[\frac{\pi}{4}\left(\pm i - \frac{|cE|}{S}\right)\right] . \quad (36)$$

Note the appearance of the exponentially small factor which represents the tunneling of the solution out of the nonlinear well. The exponent is $x_T(-E)^{1/2}$ which is the barrier width times the square root of its height. The modon is confined by virtue of its effective energy level $E$ being negative, since $E = k_y v_d/\omega - 1 - k_y^2$ and $\omega = k_y c$ .

In the radiation region $x \gg x_T$ the field can be obtained from Eq. (33b):

$$\phi_{k_y\omega}(x) = \mathcal{A}_{k_y\omega} \left|\frac{c}{Sxv_d}\right|^{1/2} \exp\left(\pm\frac{i}{2} S \left|\frac{v_d}{c}\right| x^2\right) . \quad (37)$$

Causality implies that energy is flowing to large $|x|$ and thus, the group velocity should have the sign of $x$ . This condition implies that we use the $\pm$ sign in the above equations for $ck_y \lessgtr 0$ , respectively.

The rate of energy loss of the solitary drift wave can be computed using Eq. (13a). It is valid to neglect the nonlinear radiation terms as in Eq. (13a) since $\phi$ is exponentially small for $x \gg a$ . Evaluating the energy loss using Eq. (36) and Parseval's theorem gives

$$\frac{dE_s}{dt} = -\frac{|c|L_c}{\pi v_d}\int_{-\infty}^{+\infty} dk_y |k_y| \left|\mathscr{L}_{k_y\omega}\right|^2$$

$$= -\frac{\pi L_c |c| a^2}{v_d \beta^2} A^2 \exp\left(-\frac{\pi}{2S}\left|\frac{c}{v_d} - 1\right|\right)\int_{-\infty}^{+\infty} dk_y |k_y|$$

$$\times \left(1 + k_y^2 - \frac{v_d}{c}\right)^{1/2} \exp\left(-\frac{\pi}{2S}\frac{|c|}{v_d} k_y^2\right) . \qquad (38)$$

For $|c/v_d - 1| >> 2S/\pi$ the integral is easily performed giving

$$\frac{dE_s}{dt} = -2SL_c A^2 \left(1 - \frac{v_d}{c}\right)^{-1/2} \exp\left(-\frac{\pi}{2S}\left|\frac{c - v_d}{v_d}\right|\right) . \qquad (39)$$

For the case $|c/v_d - 1| \lesssim 2S/\pi$ , the exponential factor is of order unity indicating a breakdown of the tunneling calculation. Indeed, both the barrier height, $-E$ , and the barrier width, $x_T$ , become small in this limit for small $k_y$ .

Equation (39) implies that the modon speed changes extremely slowly so long as $c/v_d > 1 + 2S/\pi$ , but that as soon as this critical speed is reached, shear damping similar to the linear case destroys the modon. Furthermore, the ion modon ($c < 0$) is only weakly damped by this mechanism. This results because of the strong screening of the exterior potential as exemplified in the Stern limit of Eq. (25).

Nonadiabatic electron terms change the analysis in two ways for $x_0 >> x_e$ . First the potential $V(x)$ in Eq. (31) is changed by the addition of $\mathscr{L}_{k_y\omega}(x)$ . This consequently modifies the WKB solutions. Also, the electron source contributes to the change in energy as shown

in Eq. (13a). If the electron source term is due to Landau resonance, then this effect will lead to an additional damping of the modon. The operator $\mathscr{L}$ results in damping because of the factor $-\omega(\omega - \omega_{*e}) \propto -c(c - v_d)$ which is negative for allowed modon speeds. This damping effect is exponentially small in $\beta x_0/a$ .

## VI. CONCLUSIONS

Numerous observations of steady state, low frequency fluctuations with frequencies, wavelengths, and amplitudes characterized by $\omega \sim k_y v_d$ , $k_\perp \rho_s \lesssim 1$ , $k_\parallel L_n \lesssim 1$ , and $\phi = e\Phi/T_e \sim \varepsilon \equiv \rho_s/L_n$ lead us to re-examine the nonlinear partial differential equation describing drift waves. This dynamical equation is derived from the two component fluid equations assuming negligible ion pressure, weak electron non-adiabaticity and quasi-neutrality. The plasma geometry considered is the nonuniform slab with a sheared magnetic field defined by $S = L_n/L_s$ .

We have shown that for weak shear, $S < \varepsilon$ , when the coupling to ion acoustic waves is negligible, the reduced drift wave equation admits localized, two-dimensional solutions. These solitary drift waves are equivalent to Rossby wave modons in geophysics, and are governed by the dimensionless partial differential equation first derived by Charney.[9] The Charney equation was obtained for nonlinear drift waves by Hasegawa and Mima.[7]

In addition to the $k_\parallel = 0$ solutions of Refs. 2, 3, and 4, we show that for weak shear there are nonlinear solitary drift-ion acoustic waves $\phi(x, y + \alpha z - ct)$ for general values of $\alpha = k_\parallel/k_y$ . These solitary drift waves propagate in regions complementary to the $\omega(k_y, k_\parallel)$ regions

of the linear oscillations as shown in the phase velocity diagram in Fig. 1. Electron-drift solitary waves have speeds $c > v_d$ while ion-drift solitary waves have speeds $c < 0$ .

These solitary vortices have a dipole-like core with radius a and an exponentially-screened exterior decaying as $\exp(-\beta r/a)$ , where $\beta/a = \left(1 - v_d/c\right)^{1/2}$ . When $\beta$ is small, the peak amplitude $e\Phi/T_e \simeq 1.28\ a/L_n$ occurs at $r_0 \simeq 1/2\ a$ . The energy, $E_s$ , of a solitary drift wave is of order $a^2 L_c n_e T_e (a/L_n)^2$ . For speeds $c > v_d$ there is a minimum energy for excitation given by $E_s \sim 4\pi a^2 L_c n_e T_e (\rho_s/L_n)^2$ (valid for $a \lesssim 1$) occurring at $\beta \sim 10^{-3} - 10^{-2}$ . At $\beta = 0$ where $c = v_d$ , the solitary drift wave becomes identical to a dipole vortex solution of the Euler equation. In this case, the exponential screening is replaced by $\phi \propto 1/r$ and the energy becomes infinite. Solitary vortices traveling in the ion-diamagnetic direction have energies which increase monotonically with increasing $|c|$ .

Estimating the maximum density of solitary vortices to be $n_s = 1/a^2 L_c$ gives an estimate of the maximum energy of a many-modon system. For densities larger than this, self-collisions would presumably destroy the modons. At the critical density, the energy $n_s E_s$ in solitary waves as a fraction of the plasma thermal energy, $n_e T_e$ is $n_s E_s / n_e T_e \simeq (a/L_n)^2 \sim (\rho_s/L_n)^2 \sim \varepsilon^2$ . This bound on the drift wave energy density is consistent with the free energy estimates of thermodynamics as well as experimental measurements.

In the presence of strong shear $S \gtrsim \varepsilon$ , the electron drift wave is intrinsically coupled to the ion acoustic oscillations due to the dispersion in $\alpha = k_\parallel / k_y = x/L_s$ with distance x from the $k_\parallel = 0$ rational surfaces. We have shown that the field of the solitary wave is

a quasi-bound state of a Schrödinger equation with a finite potential barrier. Well outside the core $r = a$ of the drift wave modon, the solutions are outgoing drift-ion acoustic waves. These outgoing waves radiate energy from the core to regions of ion-Landau damping as in the Pearlstein-Berk eigenmodes.[5]

In the radiation region, the sheared-field modons have an exponentially small amplitude determined by the tunneling of waves through the nonlinear potential barrier. For speeds such that $|c/v_d - 1| > S$, the outer modon scale, $a/\beta$, and the Pearlstein-Berk turning point, $x_T$, are well separated. We calculate the rate of loss of energy due to radiation obtaining the damping rate $\gamma_s \sim c_s/L_s \exp[-L_s/L_n|c/v_d - 1|]$. For speeds such that $|c/v_d - 1| \leq S$ the turning point is close to the outer scale, and we expect the damping rate to be qualitatively the same as for the linear eigenmodes with $0 < c < v_d$.

An important problem not fully treated here is the effect of nonadiabatic electron response. Naively one would expect an additional damping since the modon frequencies occur in the ranges $\omega > \omega_{*e}$ or $\omega < 0$. If, however, the modon is situated at the rational surface then nonlinear electron motion must be considered.

From our analysis we conclude that an important aspect of the nonlinear dynamics of drift waves is the occurence of solitary waves. The solitary drift waves are coherent, localized structures with cores of scale $a \sim \rho_s$, energies proportional to $a^2 L_c n_e T_e$, and exponentially small tails. The structures exist both in the shearless and sheared magnetic fields. In all cases the dynamics of the solitary wave components provides $\underset{\sim}{k}\omega$ spectral components that are complementary

to those of the linear modes. We consider the solitary drift-ion acoustic waves to be an important aspect of the steady fluctuations of the turbulent drift wave system.

## Acknowledgments

The authors are grateful to P. L. Similon, P. J. Morrison, H. Aref and M. N. Rosenbluth for helpful discussions. Also J. D. Meiss acknowledges the Geophysical Fluid Dynamics Summer School at Woods Hole (ONR Conract N0014-79-C-671) for support during the beginning of this work.

This work was supported by United States Department of Energy Contract No. DE-FG05-80ET-53088.

## Appendix: Ertel's Theorem

The ion fluid equation [Eq. (3)] with finite pressure terms can be rewritten in terms of the vorticity $\underset{\sim}{\omega} = \nabla \times \underset{\sim}{v}$ :

$$\frac{D}{Dt}(\underset{\sim}{\omega} + \underset{\sim}{\Omega}) + (\underset{\sim}{\omega} + \underset{\sim}{\Omega})\nabla \cdot \underset{\sim}{v} = (\underset{\sim}{\omega} + \underset{\sim}{\Omega}) \cdot \nabla \underset{\sim}{v} , \tag{A.1}$$

providing $\nabla n \times \nabla p = 0$ (the fluid is "barotropic"). Substitution of the density equation for $\nabla \cdot \underset{\sim}{v}$ in (A.1) reduces it to

$$\frac{D}{Dt}\left(\frac{\underset{\sim}{\omega} + \underset{\sim}{\Omega}}{n}\right) = \left(\frac{\underset{\sim}{\omega} + \underset{\sim}{\Omega}}{n}\right) \cdot \underset{\sim\sim}{\nabla v} \tag{A.2}$$

where n is the total electron density. Suppose there exists some scalar quantity conserved for each fluid element:

$$\frac{D\lambda}{Dt} = 0 , \tag{A.3}$$

then Ertel's theorem[8] states that the potential vorticity

$$\Pi = \frac{\underset{\sim}{\omega} + \underset{\sim}{\Omega}}{n} \cdot \nabla\lambda , \tag{A.4}$$

is also conserved by the flow. For the case at hand the large toroidal magnetic field with constant direction limits consideration to two-dimensional flows in the perpendicular plane ($k_{\parallel} \to 0$) so that $\nabla\lambda = \hat{z}$ and

$$\frac{D}{Dt}\left(\frac{\omega_z + \Omega}{n}\right) = 0 \quad . \tag{A.5}$$

This equation reduces to the Charney equation [Eq. (10)] in the limit when the velocity is completely $\underset{\sim}{E}\times\underset{\sim}{B}$ , $\underset{\sim}{v} = c_s\rho_s\hat{z}\times\nabla_\perp(e\Phi/T_e)$ , so that $\omega_z = -\Omega\rho_s^2\nabla_\perp^2(e\Phi/T_e)$ and when $n = n_0(x)\exp(e\Phi/T_e)$ . Expanding Eq. (A.5) to first-order in $e\Phi/T_e \sim \mathcal{O}(\varepsilon)$ then gives Eq. (10). More generally, Eq. (A.5) includes the effects of $\nabla B$ and diamagnetic drifts and higher order nonlinearities. In geophysics, these effects are referred to as non-geostrophic (geostrophy is defined as the state where the velocity is given entirely by the $\underset{\sim}{E}\times\underset{\sim}{B}$ drift), and the Charney equation is called the quasi-geostrophic potential vorticity equation.

## References


1. J. D. Meiss and W. Horton, Phys. Rev. Lett. 48, 1362 (1982).
2. M. E. Stern, J. Mar. Res. 33, 1 (1975).
3. V. D. Larichev and G. M. Reznik, Oceanology 16, 547 (1976).
4. G. R. Flierl, V. D. Larichev, J. C. McWilliams, and G. M. Reznik, Dyn. of Atmos. and Oceans 5, 1 (1980).
5. L. D. Pearlstein and H. L. Berk, Phys. Rev. Lett. 23, 220 (1969).
6. J. D. Meiss and W. Horton, Phys. Fluids 25, 1838 (1982).
7. A. Hasegawa and K. Mima, Phys. Rev. Lett. 39, 205 (1977) and Phys. Fluids 21, 87(1978).
8. H. Ertel, Meterorolol. Zh. 59, 277 (1942) and J. Pedlosky, Geophysical Fluid Dyanmics, (Springer Verlag, New York, 1979), p. 38-42.
9. J. G. Charney, Geophys. Public. Kosjones Nors. Videnshap.-Akad. Oslo 17, 3 (1948).
10. A. Hasegawa, C. G. Maclennan, and Y. Kodama, Phys. Fluids 22, 2122 (1979).
11. V. I. Arnold, Proc. Acad. Sci. USSR 162, 773(1965) and V. I. Arnold, Mathematical Methods of Classical Mechanics, (Springer Verlag, New York, 1978), Appendix 2J.
12. J. C. McWilliams, G. R. Flierl, V. D. Larichev, and G. M. Reznik, Dyn. Atmos. & Oceans 5, 219 (1981).
13. J. C. McWilliams and N. J. Zabusky, Geopys. & Astrophys. Fluid Dyn. 19, 207(82); also M. Makino, T. Kamimura, and T. Taniuti, J. Phys. Soc. Jap. 50, 980 (1981).

14. H. Aref, Coherent Features by the Method of Point Vortices, Geophysical Fluid Dynamics 1980 Summer Study Program, WHOI-80-53, Woods Hole Oceanographic Institute, p. 223, 1980.

15. G. K. Batchelor, An Introduction to Fluid Mechanics, (Cambridge University Press, Cambridge, U. K., 1967), Ch. 7.3.

## Figure Captions

1. Allowed speeds for the modon solution, from Eq. 20, are the shaded regions. Linear drift modes have phase speeds in the unshaded region.
2. Inner modon scale, $\gamma$ , as a function of $\beta$ through Eq. 23. The first three roots are shown.
3. Modon size and peak amplitude $\phi_s$ as a function of $\beta$ . In Fig. (3a) the graph applies for arbitrary a providing $\beta$ is given by Eq. (21). For Fig. (3b) $a = \rho_s$ .
4. Wavenumber spectrum of modon for $k_y = 0$ , $a = \rho_s$ , $c = 1.5v_d$ .
5. Modon energy and enstrophy from Eq. (28) for $a = \rho_s$ as a function of speed.

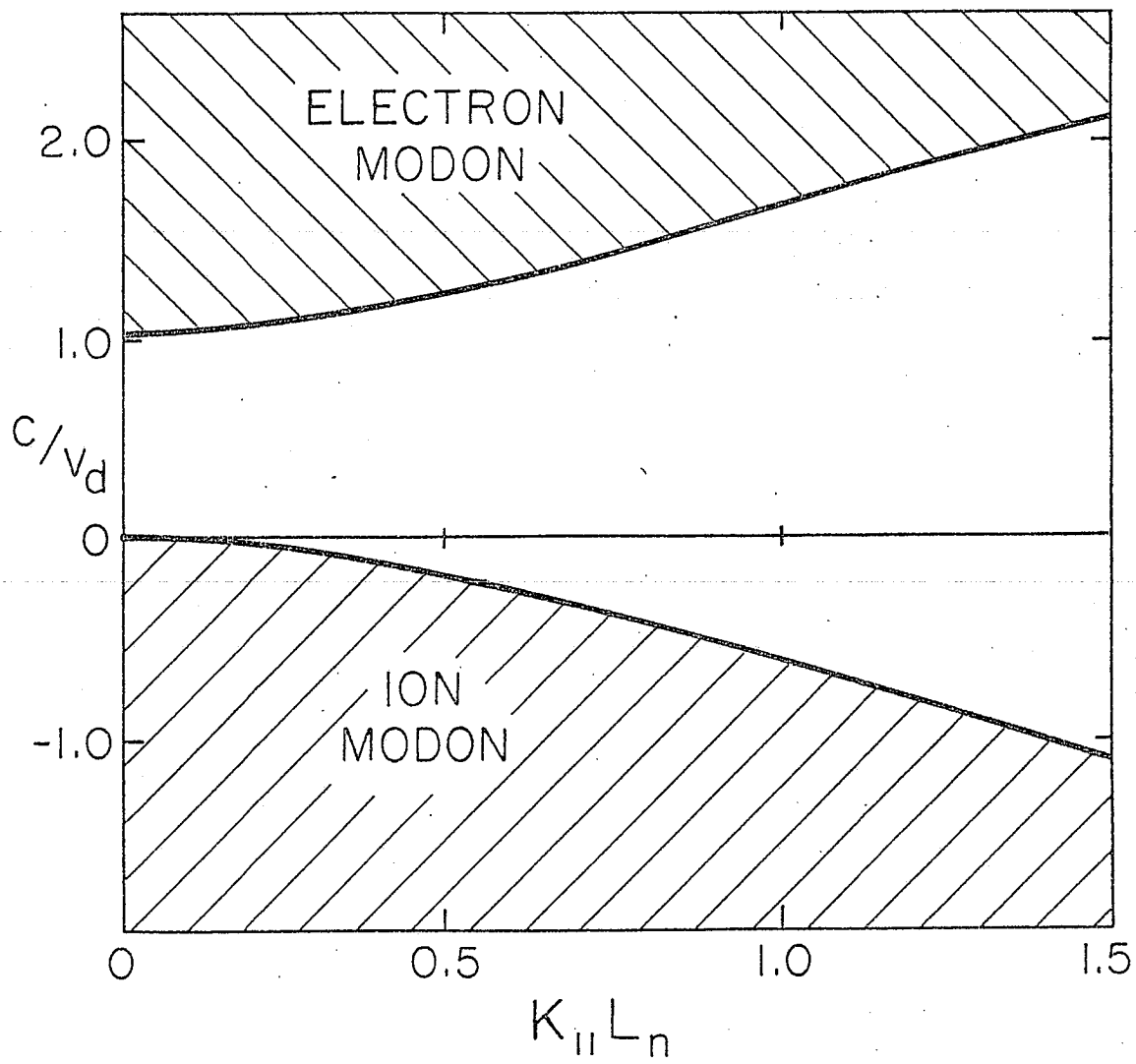


FIG. 1

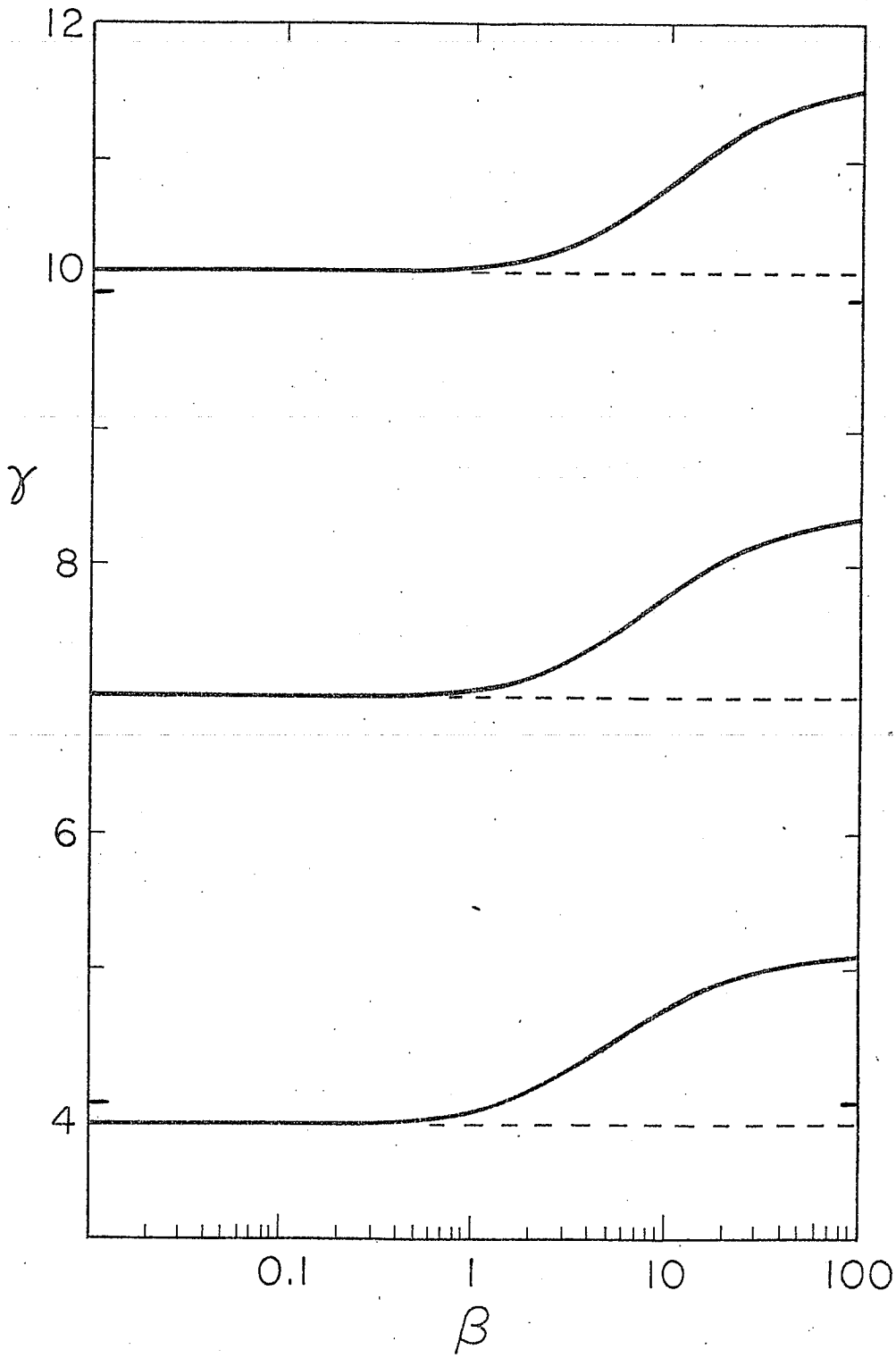


FIG. 2

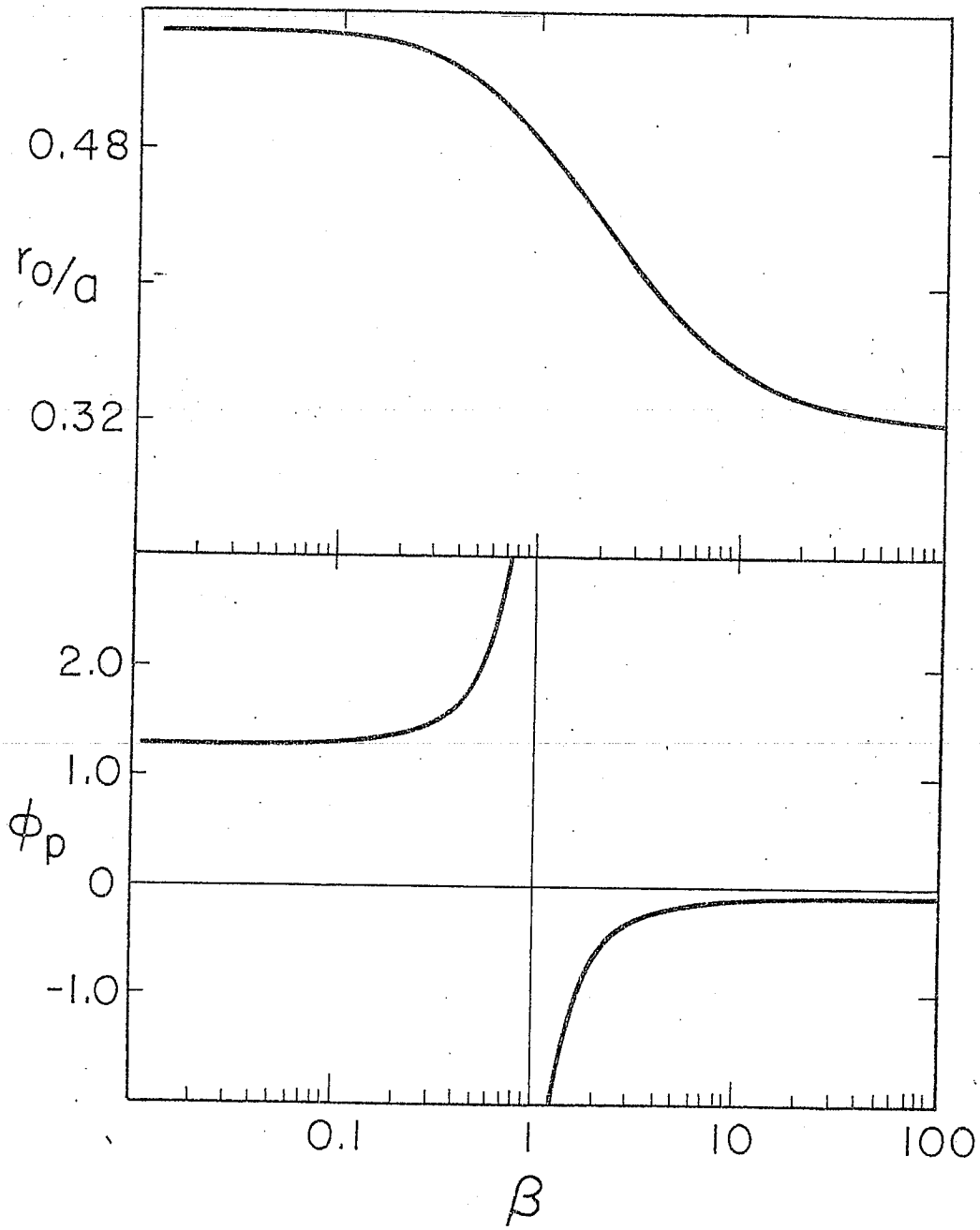


FIG. 3

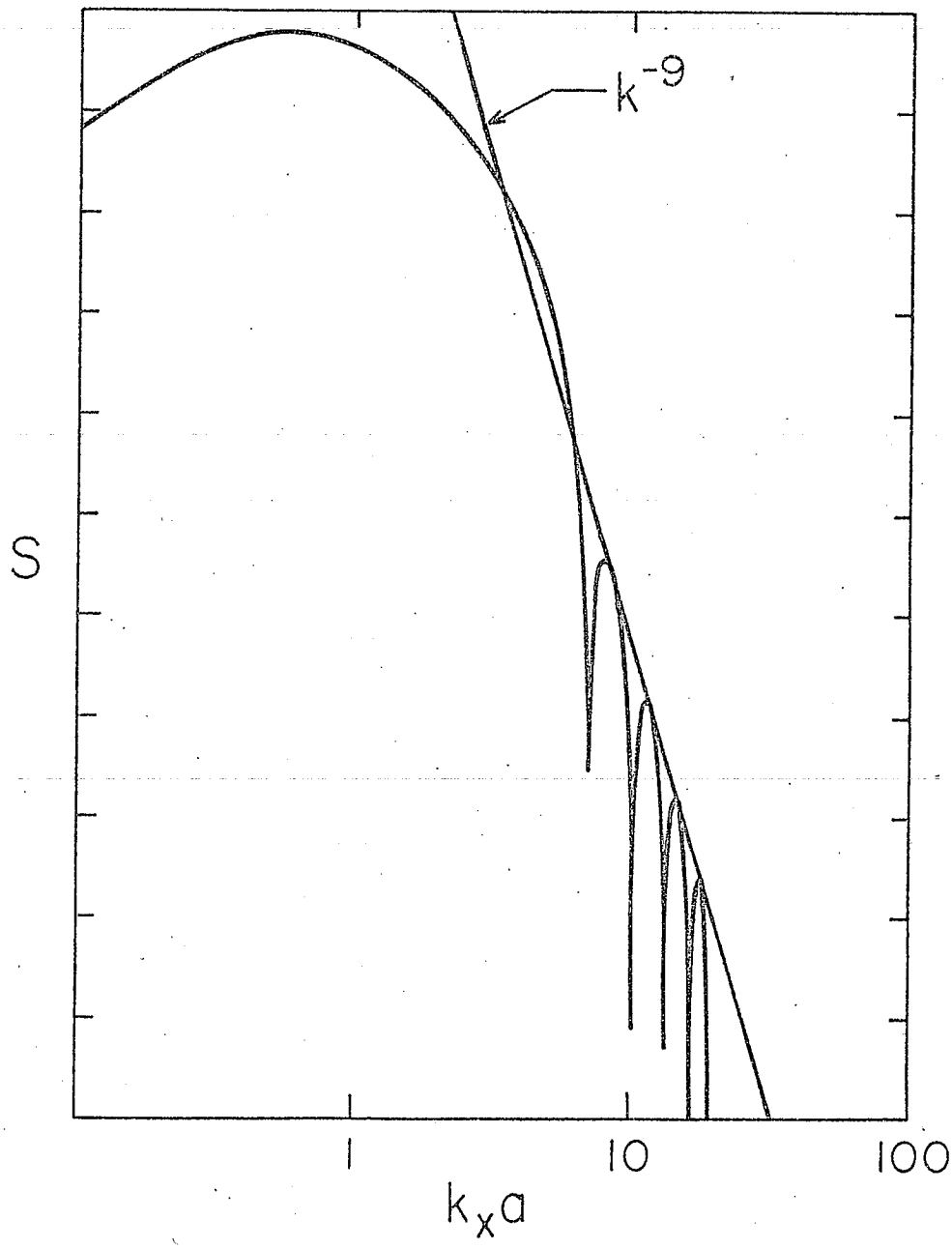


FIG. 4

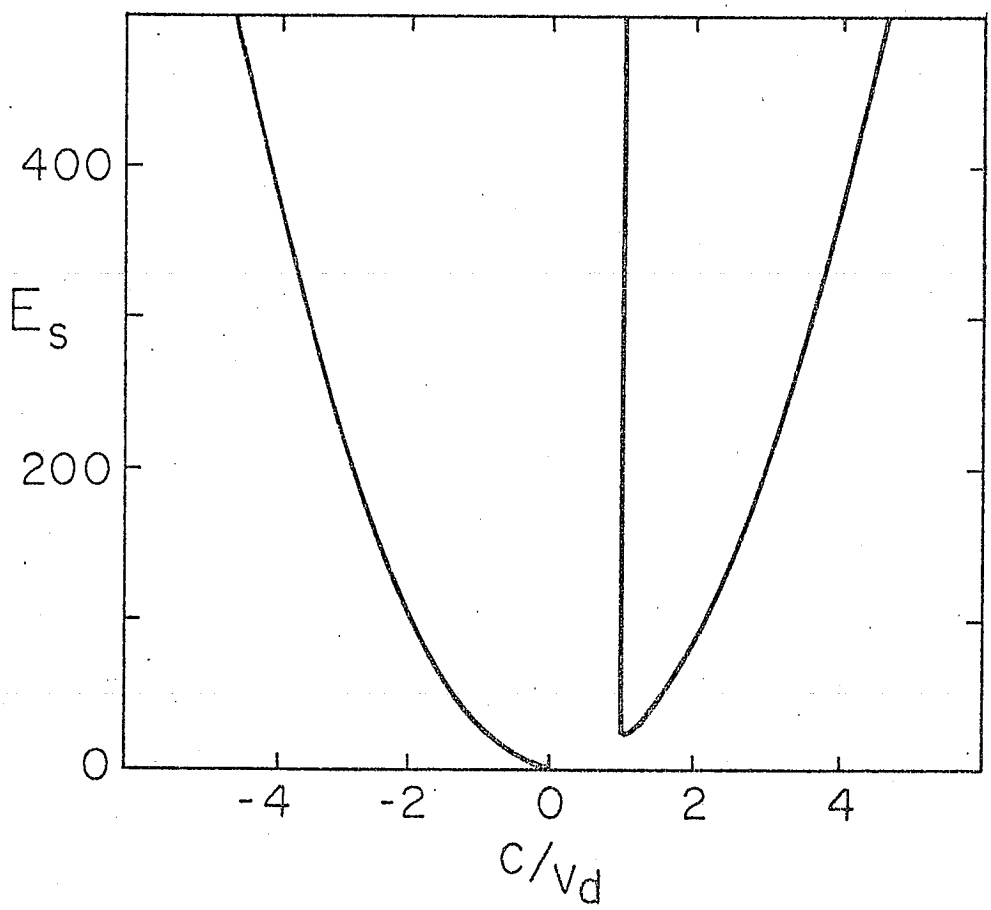


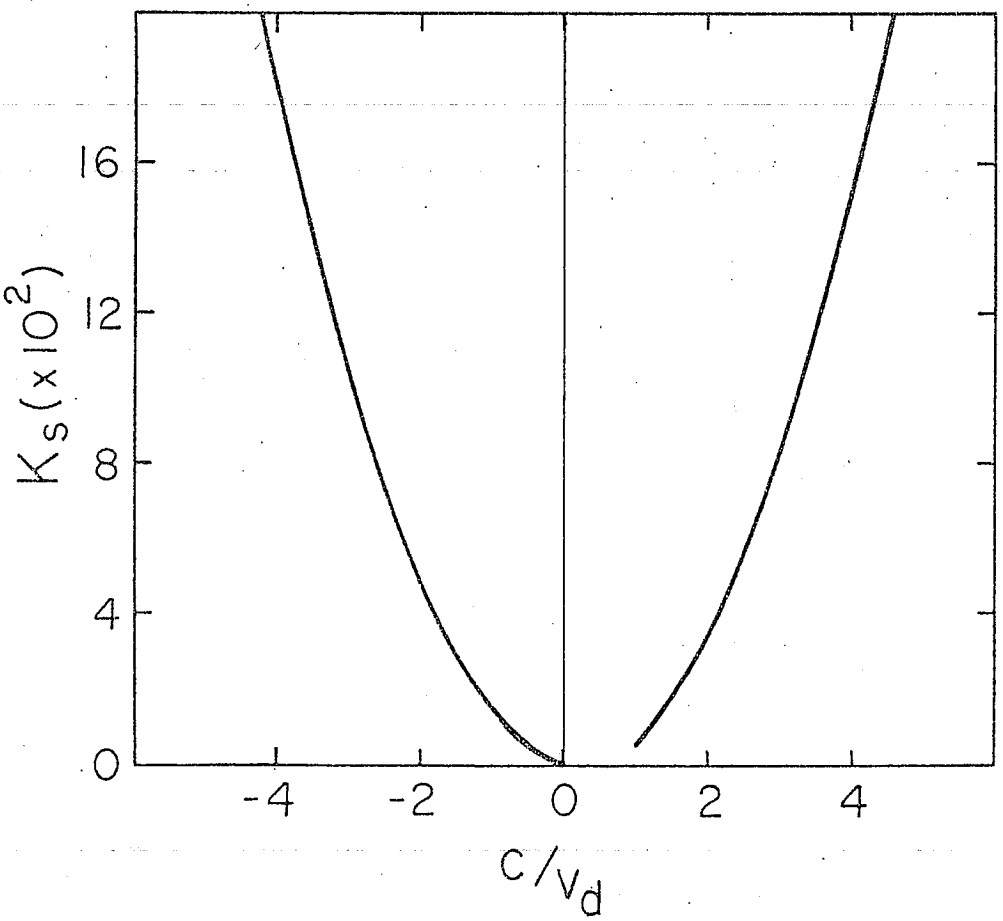


FIG. 5